a few decays per molecule must occur before the sample can be visualized. This means that, unless the investigator has extraordinary patience, a short-lived isotope must be used. Even more serious is the problem that an appreciable fraction of the atoms of the molecule must be substituted with radioisotope.

Suppose one wanted to observe a DNA of the size of *E. coli* DNA (molecular weight $\sim 2 \times 10^9$). A thousand well-spaced decays should clearly define the contour of the molecule. If ^{32}P is used, with a half life of 14 days, and one were willing to wait 14 days, then 2,000 ^{32}P atoms would have to be incorporated per molecule. This works out to a specific radioactivity of about 2.5 curies (mmole P)$^{-1}$. (One curie is 2.2×10^{12} dpm.) This is quite a high density of radiation. The sample would be prepared by allowing *E. coli* to grow on a source of ^{32}P. One must worry not only about radiation damage to the organism but also about damage to the DNA itself, which might break the molecule. Molecular autoradiography is even more difficult with higher organisms, because they are more sensitive to radiation.

In spite of these difficulties, autoradiography has been a powerful adjunct to studies on DNA. One example of its usefulness is that ^{32}P can be preferentially incorporated into newly synthesized regions by pulse labeling. Thus, the structure of regions involved in replication can be specifically examined. Proteins are not as favorable for autoradiographic studies, because the atoms they contain are not easy to substitute extensively with short-lived radioisotopes.

X-ray diffraction

X-ray diffraction is such an important technique that it is treated in detail separately in Chapters 13 and 14. Here it will be sufficient to describe the nature of some of the results obtainable from single-crystal x-ray diffraction. A successful x-ray study provides a picture of the three-dimensional electron density distribution as it repeats through the crystal lattice. One can usually conclude quite a bit about the size and probable shape of the macromolecule from the symmetry of the crystal, its density, and the size of the fundamental repeating element (the unit cell). In many cases, the number of subunits and the symmetries of their arrangement also can be obtained.

Depending on the quality of the crystal and on the extent of data collected, an electron density map is constructed with a given resolution. This governs the level of detail obtainable about the crystal structure. At 10 Å resolution, it usually will be difficult to tell where one molecule in the crystal ends and the next one begins. After all, a diameter of only 30 Å is typical for a small protein, and close contact between neighboring molecules in a macromolecular crystal is not uncommon. It is usually possible to identify the spatial distribution of electron-dense material associated with a single protein or nucleic acid at 6 Å resolution. This yields the detailed overall shape and any particularly striking features such as clefts or holes. An x-ray structure of this resolution is comparable to the very best that can be obtained from Fourier-analyzed electron micrographs of crystalline samples.

Sct 2-3

Once sufficient x-ray analysis has been done to produce an electronic density map with 4 Å or better resolution, the amount of information available about the structure reaches a level of detail unequaled by any other single technique or even by a combination of many separate techniques (except for the very similar methods of electron or neutron diffraction). At 3 to 4 Å resolution, the nature, length, and orientation of secondary-structure regions become visible. If the primary structure is known, it is usually possible to fit this into the electron density map and start to make reasonable estimates of the spatial location of each individual atom in the structure. By 2 Å resolution, the electron density map is sufficiently detailed that much of the primary structure is revealed directly from the x-ray results.

The enormous effort involved in x-ray crystallography and the need for crystalline samples means that this technique is reserved for substances of particular interest and ready availability. Nevertheless, this technique has taught us more about the structure of large molecules than any other method. It must be considered the benchmark against which the results from less definitive techniques should be tested. X-ray studies are not infallible, nor can they answer all of the questions of interest for any single protein or nucleic acid, but no other method can approach the level of structural detail attainable from a single-crystal x-ray study.

10-2 MACROMOLECULES AS HYDRODYNAMIC PARTICLES

The size and shape of a macromolecule affect its ability to move in fluid solution. Its presence also alters the bulk physical properties of the fluid. A variety of techniques can exploit these phenomena to yield estimates of the molecular weight and shape. Most of these measurements have several features in common. The level of detail inherent in the experimental data is low. Thus, physically plausible models of the molecule must be constructed and used to fit the data. Measurements in isotropic solution usually are blind to molecular asymmetry. Complicated shapes or structural features will not be resolvable. Interactions of the macromolecule with various small-molecule species in solution play an important role in determining the properties of the fluid. Limitations in the knowledge of these interactions will inevitably lead to limitations in the accuracy of the information obtainable about macromolecule structure.

A survey of techniques

The techniques to be discussed can be grouped into several categories. Translational motion dominates several experimental methods. Brownian motion in the absence of an applied force is the origin of diffusion; this can be detected by observing net transport of macromolecules, or by studying fluctuations in the number of macromolecules in a small volume element. External fields can be applied to force additional

translational motion. These fields include gravity in simple sedimentation, angular acceleration in velocity sedimentation using the ultracentrifuge, and electric fields in electrophoresis.

Rotational motion dominates other techniques. Fluorescence polarization can examine rotational Brownian motion unperturbed by external fields. EPR and NMR spectra frequently yield information about rotational motions. Here, although an external magnetic field is present, it is not a significant perturbation on the molecular motion. Flow orientation or electrical orientation can alter the normal isotropic distribution of macromolecules in a solution. Rotational motions that relax these orientations can be observed by various techniques including birefringence and dichroism. Viscosity is a measurement of the overall properties of the solution. It is markedly affected by the translational and rotational motions of dissolved large molecules.

Other techniques look essentially at fluctuations in the position or orientation of molecules. All of these contrast the various spatial distributions of macromolecules (or segments of macromolecules) within the surrounding solvent. Light scattering, x-ray scattering, and neutron scattering are fundamentally similar techniques. The kind of information available with each technique differs because of the wavelength of the radiation or particles used and the rules governing the interaction of the scattering object with the incident beam.

Macromolecular volumes and hydration

The molecular volume, V, can be easily estimated for a pure isolated molecule if the molecular weight, M, and the specific volume, $\bar{V}^{\Delta}$, of a pure sample of the substance are known.

$$V = M\bar{V}^{\Delta}/N_0 \tag{10-5}$$

N_0 is Avogadro's number. The specific volume of a pure substance is the inverse of the density. It has units of $cm^3\ g^{-1}$.

Standard methods for measuring $\bar{V}^{\Delta}$ have been known since ancient times. The weight of the sample is measured, and the volume is computed from the volume of immiscible fluid displaced when the sample is submerged. Unfortunately, the notion of a pure isolated protein or nucleic acid is not a useful one. Counterions must be present to neutralize the charge of these polyelectrolytes. Even more serious is the possibility of tight associations between normal solvent molecules (such as water) and biopolymers. The hydrated, counterion-containing macromolecule is the species actually present in measurements of aqueous solutions.

In practice, most proteins and nucleic acids are handled in approximately 0.1 M buffered salt solutions. This salt concentration is sufficient to provide ample counterion concentrations. Enormous electrostatic effects occur at much lower ionic strengths; these effects can severely affect hydrodynamic measurements. For example,

one could hardly expect to see a charged nucleic acid diffuse away from its positive counterions. The electrostatic energy needed to effect such a charge separation would be enormous. The result is that motions of large molecules and small ions will be coupled, and observed transport properties will become averages of large and small molecule properties.

At high salt concentrations, such a large fraction of the solvent is salt that one must consider a macromolecular solution to have three components: salt, water, and macromolecule. The thermodynamics of such multicomponent systems are quite complex. One must worry about preferential interactions of any two components at the expense of interactions with the third.

The complexities of both high and low ionic strength will be ignored as much as possible in the following discussion. We shall model a macromolecule solution as a two-component system of water (component 1) and macromolecule (component 2). If this were an ideal solution, the volume could be computed by adding the specific volumes of the pure separate components. For a sample with g_1 grams of water and g_2 grams of macromolecule,

$$\bar{V}_{\text{Tot}} = g_1\bar{V}_1^{\Delta} + g_2\bar{V}_2^{\Delta} \tag{10-6}$$

Unfortunately, real solutions do not show such simple behavior. Proteins and nucleic acids interact with substantial numbers of water molecules. These interactions result in nonideal solution behavior. Polar macromolecules can bind appreciable numbers of water molecules fairly tightly. Dry protein films tightly adsorb about 0.4 moles of water per mole of amino acid. One to two moles of water are bound more loosely. Data from many techniques support the idea that strong water–biopolymer interactions exist in dilute solution. For example, NMR shows a small number of very tightly bound water molecules (10 to 50 per entire protein).

Calorimetric studies show that, when a protein solution is frozen, around two moles of water per mole of amino acid (0.4 g H_2O per g protein) remain unfrozen. This water clearly is perturbed by the presence of the protein. NMR and dielectric dispersion studies find that several water molecules per amino acid have moderately restricted motions in a protein solution at room temperature. Presumably, these molecules interact with the protein often enough or tightly enough to slow down the normal rapid tumbling rates of free water molecules. How well these water molecules correspond to those seen by calorimetry is not known. There surely are weaker classes of water–macromolecule interactions that can contribute to the properties of aqueous protein solutions. Bulk water may become trapped in holes or cavities. Although not bound tightly, it will move with the protein and thus contribute to the protein's apparent size. Such water will affect hydrodynamic properties but may not show up as bound water through NMR or thermodynamic techniques.

I. D. Kuntz has developed a particularly simple technique to estimate the amount of tightly bound water. A protein solution is frozen to $-35^{\circ}C$. All of the water that freezes becomes invisible by NMR spectroscopy. Because dipolar interactions between water molecules cannot be averaged out, the spectrum of solid

water is extremely broad. Any water remaining unfrozen is still able to move sufficiently to partially average its environment and give a detectable sharp NMR signal. The number of unfrozen water molecules can be computed from the area under the spectrum. Experiments are carried out at −35°C because this leads to amounts of unfrozen water consistent with what is observable as bound water by other methods. Some examples are shown in Table 10-1.

Table 10-1
Hydration of various biopolymers: A comparison of the results from different methods

Sample	NMR-freezing	Calorimetric	Hydrodynamic[a]	Isopiestic	NMR-calculated[b]
Ovalbumin	0.33	0.32	0.14	0.30	0.37
Bovine serum albumin	0.40	~0.40	0.41	0.32	0.45
Hemoglobin	0.42	0.32	0.63	0.37	0.42
Lysozyme	0.34	~0.30	0.46	0.25	0.36
Myoglobin	0.42	—	0.45	0.32	0.45
DNA	0.59	0.61	—	0.84[c]	—

Note: Values shown are grams bound H_2O per gram anhydrous macromolecule.
[a] The average of hydrations computed by viscosity, sedimentation, and diffusion data using known axial ratios or, where these are not available, the average of self-consistent hydrodynamic hydration values such as those shown in Table 12-3.
[b] Assuming all residues to be fully hydrated, and using values derived for each amino acid residue from model compound studies.
[c] Estimated to be held by short-range interactions.

The variation in bound water in different proteins can be rationalized from the amino acid composition. Kuntz estimated the number of water molecules bound to each amino acid from studies on polypeptides. This value ranges from 6 to 7 for an anion like glutamate to only 1 for nonpolar amino acids. Such variation is reasonable because an ion will generally be tightly solvated by several water molecules, and polar groups should hydrogen-bond strongly to water, whereas a nonpolar residue can bind a water molecule only at the peptide. The amount of water one can expect to be bound to various proteins can be calculated using the hydration values for each amino acid. Agreement with experiment is quite good (as shown in Table 10-1).

Hydration treated thermodynamically

It is impractical to use such a detailed view of water–biopolymer interactions to treat the hydrodynamic properties of proteins or nucleic acids in solution. Also, there is no guarantee that tightly bound water is the sole contributor to hydrodynamic properties. Usually, a very simple model of hydration is constructed. All of the various classes of bound water are merged into a net weight of bound water per weight of macromolecule. It is assumed that this water occupies any internal spaces and also covers the surface of the polymer, smoothing any irregularities. In

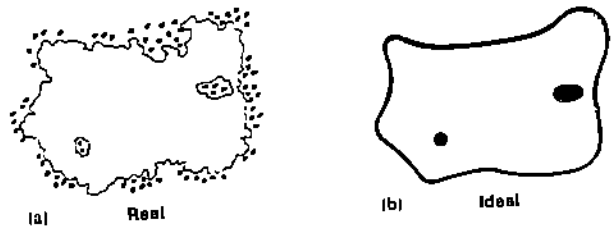

Figure 10-7
Water molecules associated with a protein or nucleic acid. (a) In reality, there are many classes of waters bound with various affinities to external and internal regions. The surface of the actual macromolecule has much fine structure. (b) In the idealization used to interpret hydrodynamic studies, the molecule's surface is smoothed, and individual bound waters are replaced by a surface film and internal pools.

return, one must admit a certain ignorance about the properties of the bound water and not look too deeply into the significance of the actual amounts needed to explain observed hydrodynamic properties. The approximations made are schematized in Figure 10-7. The real surface of a protein is extremely complicated (see Fig. 2-29).

Suppose a given macromolecule has δ_1 grams of bound water per gram of macromolecule. Let V_1^* be the specific volume of this water. If a solution consists of g_1 grams of water and g_2 grams of anhydrous macromolecule, the total volume of the solution can be computed.

$$V_{tot} = (g_1 - g_2\delta_1)\bar{V}_1^0 + g_2\bar{V}_2 + \delta_1 V_1^* g_2 \tag{10-7}$$

The first term in this equation is the volume of unbound water. It is presumed to be unperturbed and to have the same specific volume ($\bar{V}_1^0$) as pure water. The second term is the volume occupied by macromolecule. The specific volume of the macromolecule in solution ($\bar{V}_2$) is not necessarily equal to the specific volume of a pure solid macromolecule ($\bar{V}_2^0$). The third term is the volume of bound water (of specific volume V_1^*). Together, the second and third terms give the total volume occupied by the hydrated macromolecules. Because M/N_0 is the weight of a single macromolecule, it is easy to compute the volume V_h occupied by this hydrated molecule:

$$V_h = (M/N_0)(\bar{V}_2 + \delta_1 V_1^*) \tag{10-8}$$

The difficulty in using this equation is that $\bar{V}_2$, δ_1, and V_1^* are not known, nor is there any easy way to measure them. Thermodynamics can be used to resolve this dilemma by replacing these variables with others that are experimentally obtainable.

The partial specific volume of a solute, $\bar{V}_2$, is the change in solution volume when a small increment of solute is added at the limit of infinite dilution. This value is determined by measuring the density of solutions as a function of the weight concentration of solute. The expected result of such measurements can be derived

from Equation 10-7. Assuming that the macromolecular component is sufficiently dilute so that the hydration is not a function of concentration, we have

$$\bar{V}_2 = [\partial V_{tot}/\partial g_2]_{g_1,T} = -\delta_1 \bar{V}_1^{\Delta} + V_2 + \delta_1 V_1^{*} \tag{10-9}$$

Using this result, we can replace V_2 and V_1^* in Equation 10-8 to obtain

$$V_h = (M/N_0)(\bar{V}_2 + \delta_1 \bar{V}_1^{\Delta}) \tag{10-10}$$

The partial specific volume of a pure substance is equal to the specific volume. Therefore, we can replace $\bar{V}_1^{\Delta}$ in Equation 10-10 by $\bar{V}_1$, the partial specific volume of pure water. So the hydrated volume of a macromolecular solute becomes

$$V_h = (M/N_0)(\bar{V}_2 + \delta_1 \bar{V}_1) \tag{10-11}$$

Because $\bar{V}_1$ is just the inverse of the density of pure water, and $\bar{V}_2$ is measurable independently, the only unknown is the hydration (δ_1) and, as discussed above, there are numerous ways to estimate this.

In practice, partial specific volumes often are tedious to measure because of the large quantity of sample required for conventional density measurements. Accurate microbalances can alleviate these difficulties. In addition, a variety of more specialized techniques exists, including ultracentrifugation in H_2O–D_2O mixtures (Edelstein and Schachman, 1973) and density measurements using mechanical oscillators (Kratky et al., 1973). It is possible to make reasonably accurate estimates of the partial specific volumes of proteins by averaging over the amino acid composition and using estimates of specific volumes of individual amino acid residues in proteins. These estimates range from about 0.60 $cm^3\ g^{-1}$ for Asp to 0.90 $cm^3\ g^{-1}$ for Leu. A typical protein $\bar{V}_2$ is 0.73 $cm^3\ g^{-1}$, and virtually all proteins that do not contain extensive material besides amino acids have $\bar{V}_2$ values between 0.69 and 0.75 $cm^3\ g^{-1}$. Nucleic acids are much more dense, with $\bar{V}_2$ values of about 0.50 $cm^3\ g^{-1}$ if Na^+ is the counterion, or 0.44 $cm^3\ g^{-1}$ if Cs^+ is the counterion.

It is tempting to interpret Equation 10-11 by saying that $(M/N_0)\bar{V}_2$ is the volume of anhydrous macromolecule, and that $(M/N_0)\delta_1\bar{V}_1$ is the volume of bound water. However, this interpretation is hazardous. Both $\bar{V}_2$ and δ_1 contain effects due to water-biopolymer interactions. Partial specific volumes need not be equal to molecular volumes. For instance, the $\bar{V}_2$ of $MgSO_4$ is actually negative. This is because Mg^{2+} and SO_4^{2-} bind water so tightly in their hydration shells that adding $MgSO_4$ to water causes a decrease in total volume. Such electrostriction effects are not usually this dramatic in macromolecules, but they cannot be ignored.

When measured NMR hydrations are used in Equation 10-10, values of the hydrated molecular volume (V_h) are predicted that agree (in most cases) with results

from hydrodynamic measurements. In these cases, it is probable that $(M/N_0)\bar{V}_2$ is a good estimate of the anhydrous volume. Another procedure is to compute the anhydrous molecular volume from known protein crystal structures. Kuntz has shown that the value for carboxypeptidase is within a few percent of that predicted by $(M/N_0)\bar{V}_2$.

Hydrations of 0.3 to 0.4 g H_2O (g protein)$^{-1}$ are needed to account for the hydrodynamic behavior of typical globular proteins. It is instructive to estimate the added size this water represents. Consider a solid spherical protein of 30,000 mol wt. If $\bar{V}_2$ is 0.72 $cm^3\ g^{-1}$, the anhydrous molecular volume will be 3.6×10^4 Å^3. A hydration of 0.34 g H_2O (g protein)$^{-1}$ will lead to an additional volume of 1.7×10^4 Å^3 because the specific volume of water is very close to 1 $cm^3\ g^{-1}$. Suppose that all of this water exists as a spherical shell on the exterior of the protein. By computing anhydrous (20.5 Å) and hydrated (23.3 Å) radii as simply $(3V/4\pi)^{1/3}$, it is easy to show that the thickness of the spherical hydration shell will be about 2.8 Å. This is equivalent to a shell only one water molecule thick. At least qualitatively, the idea that hydration is surface-bound water has some credence.

Frictional properties of macromolecules in solution

To understand various hydrodynamic measurements—such as sedimentation rates, diffusion, or viscosity—one must be able to explain the motions of the molecules in fluid solution. These motions are much slower than gas-phase motion because of frictional forces between molecules in a condensed phase. In a hypothetical experiment, suppose an external force F is applied to a molecule with mass m. The equation of motion in a vacuum would be $\mathbf{F} = m\mathbf{a} = m(d\mathbf{v}/dt)$, where v is the velocity. In a real fluid, however, any moving particle will be subjected to frictional drag. As long as the motion is not fast enough to cause turbulence, the drag is proportional to the velocity. The resulting equation of translational motion is

$$\mathbf{F} - f\mathbf{v} = m(d\mathbf{v}/dt) \tag{10-12}$$

Here the frictional force, $f\mathbf{v}$, is shown opposing the applied force. The parameter f is called the translational frictional coefficient. It is a function of the nature of the fluid.

The linear differential equation for motion in a fluid is easy to solve. If the velocity of the macromolecule at time zero is $\mathbf{v}_0$ parallel to the applied force, and F is constant, the result is

$$\mathbf{v}(t) = (\mathbf{F}/f) + [\mathbf{v}_0 - (\mathbf{F}/f)]e^{-ft/m} \tag{10-13}$$

This solution has two important consequences. The particle is accelerated for a short time after the external force is applied. The velocity decays exponentially from the initial value $\mathbf{v}_0$ to a constant final value. This final value, $\mathbf{v}(\infty) = \mathbf{F}/f$, is linear in the applied force.

The rate of approach to a constant velocity is very rapid. For a typical macromolecule of 30,000 mol wt, f is of the order of 5×10^{-8} g sec^{-1}, and m is 5×10^{-20} g. Therefore, the transient $e^{-ft/m}$ term in Equation 10-13 decays on the time scale of 10^{-12} sec. This is the same as the time it takes molecular vibrations to relax.

In the simplest view, frictional forces arise in a fluid because of attractions among the molecules of the fluid. In order to push a solid object through the fluid it is necessary to also move some solvent molecules with respect to others (Fig. 10-8a). Solvent molecules nearest the moving particle will be most perturbed (shown as longest arrows). The disturbance caused by the particle will diminish as one moves away from it in the fluid.

To compute the frictional force, we must calculate the force required to maintain the perturbed velocity distribution of solvent molecules. This force can be phenomenologically related to a property of the fluid called the viscosity. Consider a fluid bounded by two surfaces (Fig. 10-8b). It is reasonable to postulate that the force required to slide one surface past another should be proportional to the area of the sheets (A) and should reflect the difference in velocity. If we consider the surfaces to be sheets of fluid, then for small enough velocity increments (or sheets of fluid close enough together), only the first derivative of the velocity should matter. Then,

$$F = A\eta(dv/dz) \tag{10-14}$$

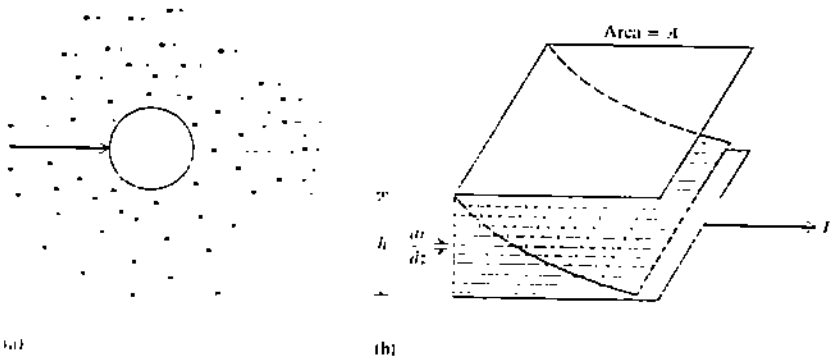

Figure 10-8

Fluid motion induced by macroscopic motion. (a) Net motions of individual water molecules, induced by a moving macromolecule. Individual erratic motions of water molecules due to Brownian motion have been neglected. (b) Distribution of fluid velocities generated by moving one parallel plane relative to another. The fluid velocity gradient, dv/dz, will be a constant if h is small, or if the relative velocity of the two planes is small. In general, however, the velocity profile need not be linear.

In this equation, η is a proportionality constant called the coefficient of viscosity. It should depend only on properties of the fluid. The velocity gradient normal to the direction of flow, dv/dz, is called the shear.

Relationship between friction and molecular size

We need to find, for the motion of a spherical particle, an equation that relates the coefficient of translational friction, f, to the fluid viscosity, η. The actual derivation is extremely complicated because one must calculate explicitly how particle motion induces velocity gradients in the fluid. Fluid mass must be conserved but, in a real case, particle motion could lead to fluctuations in the density of the fluid. It takes pages of algebra to derive an equation for the frictional coefficient of a spherical particle. However, the form of the equation can be found by dimensional analysis. The only obvious variable for the spherical particle is its radius, r. One can postulate that f is a function of η and r. The simplest possible functional form is

$$f \propto \eta^x r^y \tag{10-15}$$

The dimensions of f are g sec^{-1}; from Equation 10-14, η must have dimensions of g cm^{-1} sec^{-1}; r has dimensions of cm. Therefore, in terms of dimensions, Equation 10-15 can be written as

$$\text{g sec}^{-1} = \text{g}^x \text{cm}^{-x} \text{sec}^{-x} \text{cm}^y \tag{10-16}$$

The only values of x and y that make Equation 10-16 dimensionally correct are are $x = y = 1$. Thus, $f = \text{const}\ \eta r$.

The value of the constant cannot be determined by dimensional analysis. It depends on the boundary conditions of fluid flow at the surface of the particle. Two extreme cases usually are considered. If the particle interacts strongly with fluid molecules, it is likely that the layer of fluid immediately adjacent to the particle surface moves at exactly the same velocity as the particle. This case is called stick boundary conditions. The resulting friction equation is called Stokes law.

$$f_{sph} = 6\pi\eta r \tag{10-17}$$

At the other extreme, suppose there is no interaction between particle and fluid molecules. It is reasonable that this case should lead to weaker frictional forces. The fluid simply slips by the particle. These slip boundary conditions yield $f_{sph} = 4\pi\eta r$.

All of the preceding discussion deals with translational friction. Similar considerations apply for the damping of rotational motions of particles by viscous fluids.

If a constant torque τ is placed on a particle in a fluid, the particle will reach a constant angular velocity, ω, after a transient period. The parameter relating the velocity to the torque is the rotational frictional coefficient, $f_{rot} = \tau/\omega$. It turns out that, for stick boundary conditions, the rotational frictional coefficient of a sphere is

$$f_{rot} = 6\eta V \tag{10-18}$$

where V is the volume. For slip boundary conditions, f_{rot} of a sphere is zero. This is reasonable, because a rotating sphere will not disturb the fluid if solvent molecules do not interact with it.

A third hydrodynamic case of interest is the effect of spherical particles on the external force needed to maintain a constant velocity gradient (shear) within a fluid. We will not go into a detailed discussion of this because it is mathematically quite formidable. However, it is useful to remember that the critical variable is the volume of the macromolecular particles.

It is interesting to examine the actual distribution of solvent velocities around a dissolved molecule (for translation and rotational motion) and around a molecule suspended in a velocity gradient. Figure 10-9 shows results of detailed hydrodynamic calculations. Here the fluid velocity near the macromolecule is plotted as contours that show the change in velocity from that of the macromolecule to that of unperturbed bulk fluid. The critical thing to note from this figure is that the disturbance caused by the particle dies off very quickly with distance.

For stick boundary conditions, a substantial amount of the disturbance takes place within a thickness corresponding to the dimensions of only a single water molecule. This is a very disturbing result. The surface of a macromole is not described very well by a smooth sphere. It might appear that details of the surface would have to be taken into account for accurate hydrodynamic predictions. Furthermore, it is hard to be comfortable about a macroscopic choice of stick boundary conditions when only a single layer of water molecules is involved. Some slip boundary must be involved also. This will lead to a smaller fluid perturbation, because the difference in velocity between the bulk fluid and the macromolecule surface is smaller.

Fortunately, the effects of the roughness of the surface and the lack of pure stick boundary conditions work in opposite directions. Thus, it is customary to make the approximation summarized schematically in Figure 10-7. Hydration is assumed to add to the volume of a macromolecule without changing its shape. Stick boundary conditions are used, and any roughness of the surface is ignored. Equations 10-17 and 10-18 are used to calculate the frictional coefficients of a sphere, except that one must use a radius or volume appropriate for the hydrated particle (Eqn. 10-11). Thus, for a hydrated spherical macromolecule with a volume V_h, the expected frictional coefficients should be $f_{sph} = 6\pi\eta(3V_h/4\pi)^{1/3}$ and $f_{rot} = 6\eta V_h$.

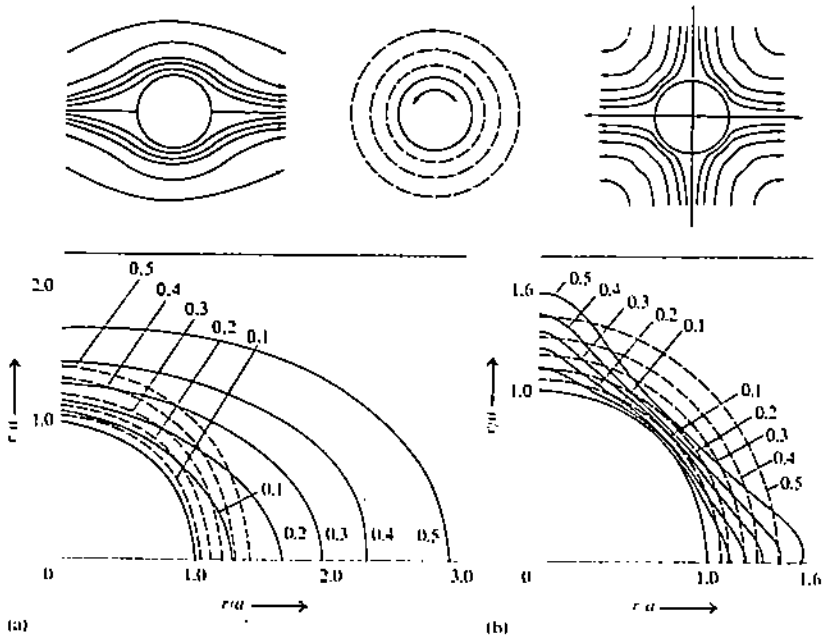

Figure 10-9

Calculated fluid velocity profile generated near a spherical macromolecule obeying stick boundary boundary conditions. In each case, a frame of reference has been chosen to make the macromolecule stationary. A cross section of the fluid, coincident with the center of the macromolecule, is shown at the top; at the bottom, just one quadrant is shown in an expanded view. Fluid velocities are shown as contour lines. Those at the bottom are labeled with the fractional velocity of the unperturbed bulk fluid. The radius of the macromolecule is a, and distance is expressed in units of a. (a) Solid lines represent a sphere moving from left to right in the fluid plane. Dashed lines represent a sphere rotating about an axis perpendicular to the fluid plane. (b) Dashed lines represent a sphere rotating about an axis perpendicular to the fluid plane. Solid lines represent a sphere in a fluid with a linear velocity gradient oriented at 45°, as indicated at the upper right. [After J. D. Kuntz, Jr., and W. Kauzmann (1974).]

For molecules the size of proteins in aqueous solution, the predictions made by employing these assumptions usually are in fairly good agreement with experiment. Much larger discrepancies can arise for smaller molecules or for less-strongly-interacting solvents. When motions of nonpolar molecules within lipid bilayers are considered, one must begin to pay serious attention to the choice of boundary conditions.

Effects of shape on translational frictional properties

Most macromolecules of biological interest are not spheres. A significant fraction appear to be compact, globular, or irregular rigid bodies. For these, an ellipsoid of revolution is a more realistic model than a sphere. There are two classes of such ellipsoids, both of which are limiting cases of the general ellipsoid with three different axes (see Fig. 10-10). The oblate ellipsoid is a disk shape, generated by rotating an ellipse around its short semiaxis b; the two long semiaxes, a, are identical. A prolate ellipsoid is a rodlike shape, generated by rotating an ellipse around its long semiaxis a; here the two shorter semiaxes, b, are identical. For either kind of ellipsoid, the axial ratio (p,) is defined as a/b, the ratio of the long to the short semiaxes.

The volume of a sphere is $(4/3)\pi r^3$, whereas that of an ellipsoid is either $(4/3)\pi a^2 b$ (oblate) or $(4/3)\pi a b^2$ (prolate). For equal volumes, the surface area of either ellipsoid will be greater than that of a sphere. It seems reasonable to guess that ellipsoids will have larger frictional coefficients than equivalent spheres, and this guess is confirmed by detailed calculations. Because the volume of a molecule is proportional to the molecular weight (Eqn. 10-11), we see that (for constant mass) the more a molecule deviates from a sphere, the larger its frictional coefficient will become.

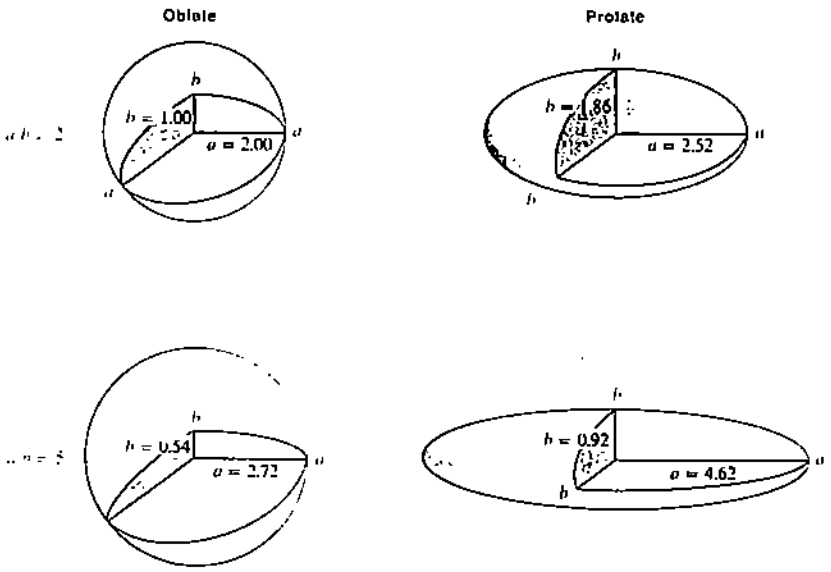

Figure 10-10

Four ellipsoids of revolution, with equal volumes. The near right octant of each ellipsoid has been cut away to show the major (a) and minor (b) axes.

For stick boundary conditions, it is possible to obtain analytical expressions for the dependence of the frictional coefficient of an ellipsoid on the axial ratio. It is useful to express these as the ratio of the frictional coefficient of an ellipsoid (f) to that of a sphere with equal volume (f_{sph}). For translational friction, the results are the following:

$$F = f/f_{sph} = (1 - p^2)^{1/2}/p^{2/3} \ln\{[1 + (1 - p^2)^{1/2}]/p\}$$

for a prolate ellipsoid, where $p = b/a = 1/p_a$ (10-19a)

$$F = f/f_{sph} = (p^2 - 1)^{1/2}/p^{2/3} \tan^{-1}[(p^2 - 1)^{1/2}]$$

for an oblate ellipsoid, where $p = a/b = p_a$ (10-19b)

These equations are not especially convenient to use; therefore, Table 10-2 lists numerical values. The translational frictional coefficient ratio F is often called a shape factor or Perrin factor. Note that the value of these factors increases rather gradually with increasing axial ratio (Fig. 10-11). Prolate ellipsoids always show a higher frictional coefficient than oblate ellipsoids of the same axial ratio. Note that,

Table 10-2
Simha (ν), Perrin (F), and Scheraga–Mandelkern (β) shape parameters for ellipsoids of revolution

Axial ratio	Prolate			Oblate		
	ν	F	$\beta \times 10^{-6}$	ν	F	$\beta \times 10^{-6}$
1	2.500	1.000	2.12	2.500	1.000	2.12
2	2.908	1.044	2.13	2.854	1.042	2.12
3	3.685	1.112	2.16	3.430	1.105	2.13
4	4.663	1.182	2.20	4.059	1.165	2.13
5	5.806	1.250	2.23	4.708	1.224	2.14
6	7.098	1.314	2.28	5.367	1.277	2.14
8	10.103	1.433	2.35	6.700	1.374	2.14
10	13.634	1.543	2.41	8.043	1.458	2.14
15	24.65	1.784	2.54	11.42	1.636	2.14
20	38.53	1.996	2.64	14.80	1.782	2.15
30	74.51	2.356	2.78	21.58	2.020	2.15
40	120.76	2.668	2.89	28.37	2.212	2.15
50	176.81	2.946	2.97	35.16	2.375	2.15
60	242.28	3.201	3.04	41.95	2.518	2.15
80	400.5	3.658	3.14	55.52	2.765	2.15
100	593.7	4.067	3.22	69.10	2.974	2.15
200	2,052.9	5.708	3.48	137.01	3.735	2.15

NOTE: F is calculated by using Equation 10-19; ν and β are calculated as described in Chapter 12 (see Eqns. 12-23 and 12-29).
SOURCE: After H. A. Scheraga, *Protein Structure* (New York: Academic Press 1961).

if there is hydration, Equation 10-19 refers to the ratio of the frictional coefficient of an ellipsoid to that of a sphere with the same *total hydrated* volume.

Effects of shape on rotational frictional properties

The frictional coefficient for nonspherical bodies is a nine-component tensor, $\underline{f}$. It was not necessary to consider this tensor in detail in the equations for the translational frictional coefficient. In most hydrodynamic measurements, one typically observes net mass transport; an explicit knowledge of the orientation of the molecule during transport is not necessary. The magnitude of the frictional coefficient observed (f) is an average over the various components of $\underline{f}$. Thus, instead of the nine parameters needed to describe $\underline{f}$, we required only the single parameter f.

However, measurements of rotational motion must include the detailed distribution of orientations. It is impossible to speak of just a single rotational frictional coefficient. There are two coefficients for ellipsoids: f_a for rotation about the a semiaxis, and f_b for rotation about the b semiaxis. By using stick boundary conditions, J. B. Perrin derived expressions for these coefficients in 1934. The rotational frictional coefficients are similar in spirit to (but much more complex than) the corresponding translational frictional coefficients of Equation 10-19. We give them here in as compact a form as possible. These frictional coefficient ratios are defined relative to the rotational frictional coefficient of a sphere of equivalent volume.

$$F_a = f_a/f_{rot} = 4(1 - p^2)/3(2 - p^2S) \tag{10-20a}$$

$$F_b = f_b/f_{rot} = 4(1 - p^4)/3p^2[S(2 - p^2) - 2] \tag{10-20b}$$

In these equations, S and p are defined as follows:

Prolate ellipsoid:
$$S = 2(1 - p^2)^{-1/2} \ln\{[1 + (1 - p^2)^{1/2}]/p\} \tag{10-21a}$$
$$p = b/a = 1/p_r \tag{10-21b}$$

Oblate ellipsoid:
$$S = 2(p^2 - 1)^{-1/2} \tan^{-1}[(p^2 - 1)^{1/2}] \tag{10-22a}$$
$$p = a/b = p_r \tag{10-22b}$$

Note the similarity of the algebraic form of the parameter S to the translational frictional coefficient ratios for ellipsoids (Eqn. 10-19). In fact $S = 2p^{-2/3}/F$.

Figure 10-11b plots the rotational frictional coefficient ratios for oblate and prolate ellipsoids. Some important qualitative conclusions are evident. Oblate ellipsoids produce roughly the same friction, whether they rotate around the long axis (f_a) or the short axis (f_b). Both motions involve more friction than does the rotation of an equivalent sphere. Prolate ellipsoids rotate around their long axis (f_a) more easily than an equivalent sphere rotates. However, rotation around their short axis (f_b) is accompanied by extremely great friction. This observation is reasonable, because such motion is bound to perturb the fluid quite considerably. (Just think of the design of a standard magnetic stirrer.)

Each of the rotational frictional coefficients can be related to a rotational relaxation time, τ_r. This variable measures the rate at which an anisotropic distribution relaxes to equilibrium through that particular rotational mode. For a sphere, $\tau_r = f_{rot}/2kT$. For ellipsoids (relative to equivalent spheres),

Prolate ellipsoid:
$$\tau_a/\tau_r = f_b/f_{rot} \tag{10-23a}$$
$$\tau_b/\tau_r = (2/f_{rot})[(1/f_a) + (1/f_b)]^{-1} \tag{10-23b}$$

Oblate ellipsoid:
$$\tau_b/\tau_r = f_a/f_{rot} \tag{10-23c}$$
$$\tau_a/\tau_r = (2/f_{rot})[(1/f_a) + (1/f_b)]^{-1} \tag{10-23d}$$

where τ_a is the relaxation time for orientation about the long axis, and τ_b for orientation about the short axis. You can rationalize these equations if you think about the motion of a prolate ellipsoid. To change the spatial orientation of the long axis (a), you must rotate about one of the two equivalent short axes (b). Rotation about a has no effect. However, to change the orientation of one of the short axes, either rotation about a or b will do, and either should be equally effective, except that the short-axis rotation will involve more friction.

Various measurements of macromolecular rotation yield parameters that are related to τ_a and τ_b but, unfortunately none of the conventional NMR, electric dichroism or birefringence, dielectric relaxation, or fluorescence polarization techniques give τ_a and τ_b directly. Some methods give τ_a and τ_b mixed in with other quantities that may not be known accurately. It is often a formidable task to sort τ_a and τ_b out of results from techniques such as fluorescence polarization. Decay of fluorescence anisotopy mixes τ_a and τ_b with a series of exponentials whose coefficients are weighted by, among other things, the orientation of the fluorescent probe with respect to the principal axes of the ellipsoid (see Chapter 8). Other methods, such as static fluorescence polarization or non-Newtonian viscosity, can yield only the harmonic mean of τ_a and τ_b. For a prolate ellipsoid $\tau_h^{-1} = 1/3[\tau_a^{-1} + 2(\tau_b)^{-1}]$, and the corresponding mean rotational frictional coefficient is $f_h = (2\tau_h)^{-1}$.

It is a shame that it is so difficult to measure τ_a and τ_b independently because, as comparison of Figure 10-11a and 10-11b clearly shows, rotational friction is a much more sensitive measure of shape than is translational friction. However, rotational frictional coefficients are also much more sensitive to the choice of boundary conditions. We have already discussed this dependence for spheres. When slip boundary conditions are used for ellipsoids, translational friction is only moderately altered. Rotation is strikingly affected. With slip boundary conditions, there will be no frictional drag for rotation about the long axis of a prolate ellipsoid or the short

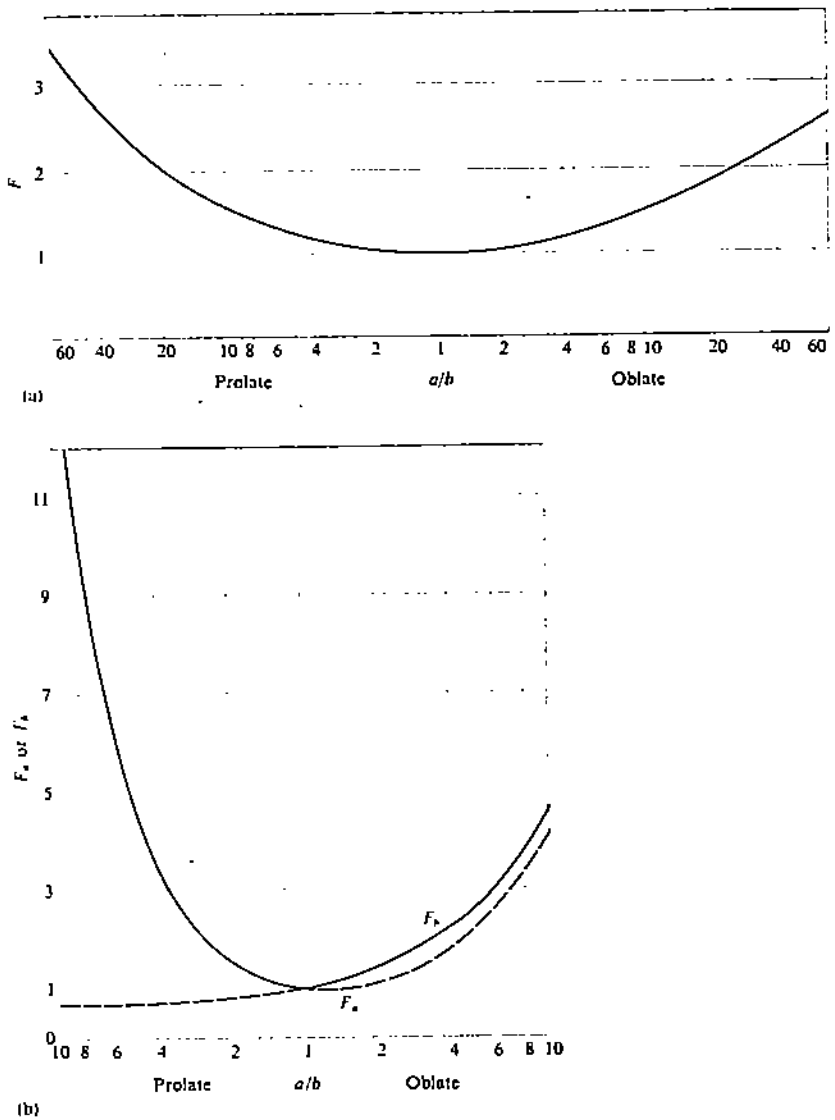

Figure 10-11

Frictional coefficients for ellipsoids, relative to those for spheres of equal volume. (a) Translational frictional coefficient ratio F, defined in Equation 10-19. (b) Rotational frictional coefficient ratios F_a and F_b, defined in Equation 10-20. The ratio F_b is for rotation around the short axis; F_a is for rotation around the long axis. F_a approaches the value 2/3 as a prolate ellipsoid becomes infinitely long. For oblate ellipsoids, in the limit of large a/b, $F_a = F_b = 3a/4\pi b$. [After S. Koenig. *Biopolymers* 14:2421 (1975).]

axis of an oblate ellipsoid. In contrast, rotation about the other axes involves more and more friction as the axial ratio increases. Robert Zwanzig has calculated that, in the limit of long axial ratios, the frictional coefficients become the same whether stick or slip conditions are used for rotations about the nonunique axes of ellipsoids of revolution (Fig. 10-12).

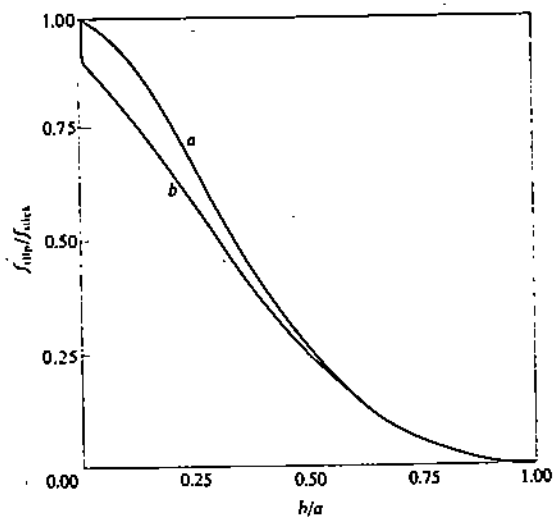

Figure 10-12

Effect of boundary conditions on the rotational frictional coefficients. Curve *a* is for rotation around the long axis of an oblate ellipsoid. Curve *b* is for rotation around the short axis of a prolate ellipsoid. Results are shown as a function of the inverse axial ratio, h/a, to allow extension of the data to infinite axial ratios. [After D. R. Bauer, J. I. Brauman, and R. Pecora, *J. Am. Chem. Soc.* 96:6840 (1974).]

Translation friction of molecules with complex shapes

In many cases, ellipsoids are unsatisfactory models for the shapes of biopolymers. In these cases, one must attempt to predict the hydrodynamic properties of more complex structures. An approximate method for computing the friction of a structure made of identical subunits was developed by J. G. Kirkwood and J. Riseman. There are two major applications of this theory. A linear or coiled polymer can be approximated as a string of beads, each with identical hydrodynamic properties. An oligomeric protein can be modeled as a cluster of identical subunits with the same hydrodynamic properties. In either case, the major problem is to deal with the hydrodynamic interaction between subunits. We will restrict our discussion to the